Tunable Tradeoff between Quantum and Classical Computation via Nonunitary Zeno-like Dynamics

P.V. Pyshkin,[1,2,3,*] A. Gábris,[4,3] Da-Wei Luo,[5] J.Q. You,[6] and Lian-Ao Wu[2,7,8,†]

[1] *Department of Physical Chemistry, The University of the Basque Country UPV/EHU, Bilbao 48080, Spain*
[2] *Department of Physics, University of the Basque Country UPV/EHU, Bilbao 48080, Spain*
[3] *Institute for Solid State Physics and Optics, Wigner Research Centre, P.O. Box 49, Budapest H-1525, Hungary*
[4] *Czech Technical University in Prague, Faculty of Nuclear Sciences and Physical Engineering Břehová 7, 115 19 Praha 1, Staré Město, Czech Republic*
[5] *Center for Quantum Science and Engineering and Department of Physics,Stevens Institute of Technology, Hoboken, New Jersey 07030, USA*
[6] *Department of Physics and State Key Laboratory of Modern Optical Instrumentation, Zhejiang University, Hangzhou 310027, China*
[7] *IKERBASQUE Basque Foundation for Science, 48013 Bilbao, Spain*
[8] *EHU Quantum Center, University of the Basque Country UPV/EHU, Leioa, Biscay 48940, Spain*

(Received 24 November 2020; revised 31 December 2021; accepted 19 September 2022; published 25 October 2022)

We propose and analyze a nonunitary variant of the continuous time Grover search algorithm based on frequent Zeno-type measurements. We show that the algorithm scales similarly to the pure quantum version by deriving tight analytical lower bounds on its efficiency for arbitrary database sizes and measurement parameters. We also study the behavior of the algorithm subject to noise, and find that under certain oracle and operational errors our measurement-based algorithm outperforms the standard algorithm, showing robustness against these noises. Our analysis is based on deriving a non-Hermitian effective description of the algorithm, which yields a deeper insight into components responsible for the quantum and the classical operation of the protocol.

DOI: 10.1103/PhysRevApplied.18.044060

I. INTRODUCTION

Quantum measurement has been proven to be a powerful tool that not only allows us to learn about a quantum system but also to control its state. It plays a fundamental role in quantum information with applications, among many other things, ranging from quantum communications to quantum algorithms. The quantum Zeno effect (QZE) is a widely employed technique for quantum control, which is based on repeated frequent measurements of the entire system or part of it [1]. A number of studies have employed the QZE or similar techniques for various flavors of search problems [2–4], to establish remarkable relations between the efficiency of quantum and associated classical algorithms [5], as well as singular value transformations [6]. The Zeno dynamics of a closed quantum system induced by projective measurement will yield unitary dynamics, but the evolution due to observation may be more general. Measurement-induced nonunitary dynamics have been considered in the literature both as primitives [7–11], or as essential ingredients of specific protocols [12–23]. Another source of nonunitary evolution may be a special coupling with environment [24–26].

In this paper, we consider an algorithm that is a variant of the continuous-search algorithm introduced by Farhi and Gutmann [27]. This algorithm follows a scheme based on the combination of time-dependent measurement and Hamiltonian evolution of the system [12], admitting a nonunitary description and exhibiting a nonperiodic time dependence of the target fidelity. Our approach is based on repeated measurements and postselection, therefore the survival probability associated with successfully completing the desired number of steps may be less than one, in addition to the usual probability related to the target fidelity. We show that in the case of a detuned oracle, the target fidelity can be increased up to unity at the expense of the survival probability, which makes it a favorable choice in situations where the correctness of the obtained result cannot be easily verified. While the algorithm is interesting in its own right, it is remarkable that our measurement-based algorithm is robust and self-protected against a certain class of noises [28,29]. This robustness can be attributed to the noise suppression of the repeated

*Corresponding author. pavel.pyshkin@gmail.com
†lianaowu@gmail.com

measurements. The algorithm provides a framework for studying the tradeoff between quantum and classical computation, where the quantum speedup is related to the unitary operations while measurements lead to the appearance of classical probabilities for different outcomes. Thus, in order to combine classical and quantum computations in a single process, one can consider unitary dynamics interrupted by selective measurements.

II. THE ALGORITHM

We start from the continuous-time Grover search algorithm described by the Hamiltonian in the Hilbert space $\mathcal{H}_N$ ($\dim \mathcal{H}_N = N$),

$$H_G = H_o + H_d = -|w\rangle\langle w| - |s\rangle\langle s|, \tag{1}$$

where $|s\rangle = \sum_n^N |n\rangle/\sqrt{N}$ and $|w\rangle$ denotes the marked element in the database. Taking $|\psi(0)\rangle = |s\rangle$ as the initial state the evolution remains in a two-dimensional subspace of the total Hilbert space spanned by the basis vectors $\{|w\rangle, |r\rangle\}$, where $|r\rangle = (|s\rangle - x|w\rangle)/\sqrt{1-x^2}$, and $x = 1/\sqrt{N}$. The evolution of the initial state is given by [27]

$$|\psi(t)\rangle = e^{-iH_G t}|s\rangle = e^{it}\Big\{\big(x\cos(xt) + i\sin(xt)\big)|w\rangle + \sqrt{1-x^2}\cos(xt)|r\rangle\Big\}, \tag{2}$$

where we take $\hbar = 1$ for convenience. As follows from Eq. (2) the probability to have the system in the target state $|w\rangle$ oscillates in time, with maxima at $T_j = \pi x^{-1}(1/2 + j) \propto \sqrt{N}$, where $j = 0, 1, 2, \ldots$. This periodic behavior is a consequence of the unitarity of the evolution. We stress here that the issue of this periodic behavior can also be tacked by adiabatic quantum search algorithms [30,31], as well as sophisticated time-dependent protocols [32,33].

It is well known that the nonunitary dynamics of quantum systems can have an asymptotic steady state instead of nondamping oscillations (see, e.g., Ref. [13,14,16,17]). We design a modification of this algorithm so that $|w\rangle$ becomes such a steady state.

Let us introduce our nonunitary protocol. We add a qubit ancilla to our system and extend its Hamiltonian to

$$H = -\mathcal{I} \otimes |w\rangle\langle w| - \sigma_z \otimes |s\rangle\langle s|, \tag{3}$$

with $\mathcal{I}$ and σ_z being the identity and Z-Pauli matrices acting in a space $\mathcal{H}_A = \{|\uparrow\rangle, |\downarrow\rangle\}$ of the ancilla qubit. Thus the joint Hilbert space now is $\mathcal{H}_A \otimes \mathcal{H}_N$. We underline here that the interaction between oracle and ancilla "does not know" about $|w\rangle$ state.

We consider the continuous evolution interrupted by projective measurements. The nth step of the protocol of nonunitary evolution is the following:

(1) The initial state of joint system is $|q_{n-1}\rangle \otimes |\psi_{n-1}\rangle$, where ancilla state $|q_{n-1}\rangle = \cos\theta_{n-1}|\uparrow\rangle + \sin\theta_{n-1}|\downarrow\rangle$

(2) The joint system evolves time δt driven by Hamiltonian (3). It is worth noting that δt is not necessarily small, but we assume $\delta t \ll T_0$.

(3) One performs projection measurement $|q_n\rangle\langle q_n|$ on the ancilla, where $|q_n\rangle = \cos(\theta_{n-1} + \delta\theta)|\uparrow\rangle + \sin(\theta_{n-1} + \delta\theta)|\downarrow\rangle$, where $\delta\theta = \alpha x \delta t \ll 1$, with α being a tunable parameter.

(4) A successful outcome occurs with probability p_n, and one leaves the state of joint system in the state $|q_n\rangle \otimes |\psi_n\rangle$. Otherwise, an unsuccessful outcome indicates that this run of the algorithm must be aborted.

(5) Let $\theta_n = \theta_{n-1} + \delta\theta$.

See Fig. 1 for a circuit-diagram representation of the complete algorithm. We would like to point out that the algorithm does not require reinitialization of the ancilla qubit after each measurement to some initial state, and this can be considered an advantage.

The Hamiltonian in Eq. (3) can describe single charged spin-1/2 particle on a complete graph [34] with unconstrained and spin-dependent hopping [35], with w corresponding to some unknown vertex where the electrostatic gate is applied (see Fig. 2). In such a case, Eq. (3) can be rewritten as $H = -c^\dagger_{w\uparrow}c_{w\uparrow} - c^\dagger_{w\downarrow}c_{w\downarrow} - \sum_{i\neq j}(c^\dagger_{i\uparrow}c_{j\uparrow} - c^\dagger_{i\downarrow}c_{j\downarrow})$, where $c_{i\uparrow(\downarrow)}$ is the annihilation operator for the particle on site i with spin $\uparrow$ ($\downarrow$). In this setting, the spin degree of freedom acts as ancilla.

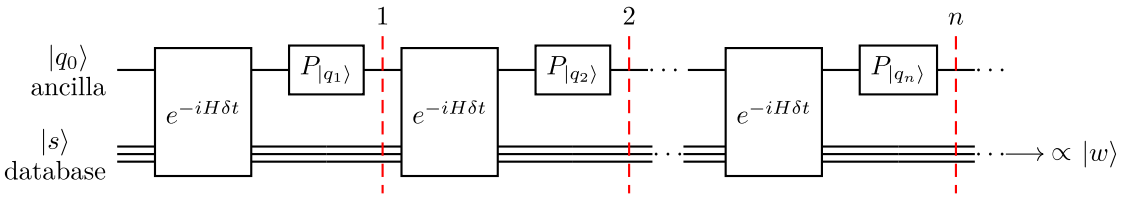

FIG. 1. Circuit diagram of the nonunitary algorithm. The ancilla states are $|q_n\rangle = \cos\theta_n|\uparrow\rangle + \sin\theta_n|\downarrow\rangle$ with $\theta_n = \theta_0 + n\delta\theta$ as defined in the text. The operation $P_{|q_n\rangle}$ denotes the projection onto the state $|q_n\rangle$ as a result of the measurement and postselection. As shown in Sec. III, the state of the database register asymptotically approaches the marked element $|w\rangle$ up to a factor reflecting the survival probability.

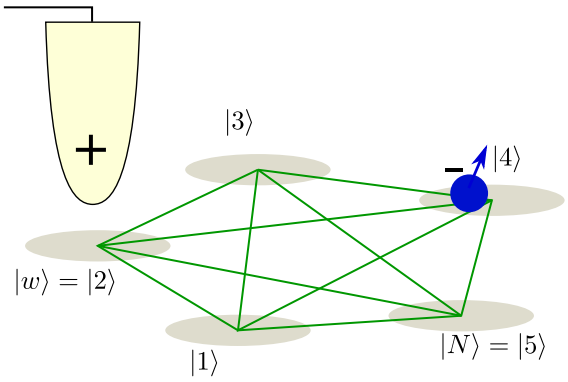

FIG. 2. Possible proof-of-concept realization of our proposed algorithm, with spin-dependent hopping of spin-1/2 particle on a complete graph. The marked node $|w\rangle$ has an additional potential (electrostatic gate). The spin degree of freedom plays the role of an ancilla qubit.

Another way to implement the Hamiltonian (3) (at least as a proof of concept) with the common quantum circuit model is to use a Trotterization technique [36–39]. In this approach we can use the Trotter formula

$$e^{-iH\delta t} = \lim_{m\to\infty} \left(e^{i|w\rangle\langle w|\delta t/m} e^{i\sigma_z|s\rangle\langle s|\delta t/m}\right)^m . \tag{4}$$

For real simulations, one should use some finite value of m in Eq. (4). In order to implement the unitary operation for the first multiplier in the round brackets (oracle) in Eq. (4) one can use the algorithm depicted in Fig. 3, while for the second one (diffusion operator) one can use the algorithm depicted in Fig. 4.

III. NONUNITARY DESCRIPTION

The stroboscopic dynamics described above corresponds to a transformation of the initial state $|s\rangle$ by a nonunitary operator $V(n)$ via

$$|\psi_n\rangle = \frac{V(n)\,|s\rangle}{\sqrt{\langle s|V^\dagger(n)V(n)|s\rangle}}, \tag{5}$$

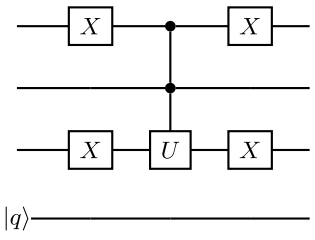

FIG. 3. Realization of the operator $\exp(i\,|w\rangle\,\langle w|\,\delta t/m)$ via the circuit model for $N = 2^3$ and $|w\rangle = |010\rangle$. Controlled unitary is $U = \mathrm{diag}(1, e^{i\delta t/m})$. The bottom wire corresponds to the ancilla qubit, which is not involved in the construction of the oracle.

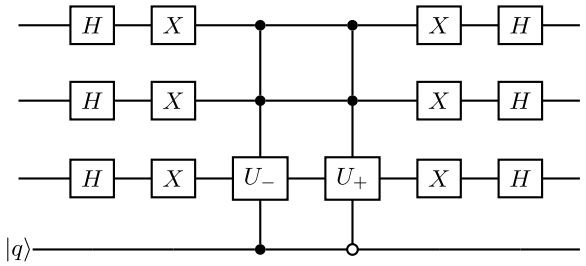

FIG. 4. Realization of the operator $\exp(i\sigma_z \otimes |s\rangle\,\langle s|\,\delta t/m)$ via the circuit model for $N = 2^3$. Controlled unitaries are $U_\pm = \mathrm{diag}(1, e^{\pm i\delta t/m})$. The bottom wire corresponds to the ancilla qubit.

where

$$V(n) = \prod_{j=1}^{n} V_j, \text{ and } V_j = \langle q_j|e^{-iH\delta t}|q_{j-1}\rangle\,. \tag{6}$$

Note, that the terms in the above product are ordered from right to left. The survival probability $P(n)$ of n first steps is hence given by $P(n) = p_1 p_2 \ldots p_n = \langle s|V(n)^\dagger V(n)|s\rangle$. Equations (5) and (6) can be considered as a set of positive operator-valued measurements (POVMs) in the Hilbert space of the oracle. One can add operators $V'_j = \langle q_j^\perp|e^{-iH\delta t}|q_{j-1}\rangle$ with $|q_j^\perp\rangle = \sin(\theta_j)\,|\uparrow\rangle - \cos(\theta_j)\,|\downarrow\rangle$ to have a full set of POVM operators for each step $\{V_j^\dagger V_j, V_j'^\dagger V'_j\}$. It is easy to check $V_j^\dagger V_j + V_j'^\dagger V'_j = \mathbb{I}$. We define the target fidelity at step n as $f\,(n) = |\,\langle w|\psi_n\rangle\,|^2$. Together with survival probability $P(n)$ these are the main characteristics of our nonunitary process.

Exact analytic calculation of $V(n)$ in Eq. (6) is difficult, however, at first we can note that Hamiltonian (3) has a block-diagonal structure and the calculation of a single δt step is an easy task. Taking $\theta_0 = 0$ we obtain the expression

$$V(n) = \prod_{j=1}^{n} \left(C_j\, e^{-i(H_o+H_d)\delta t} + S_j\, e^{-i(H_o-H_d)\delta t}\right), \tag{7}$$

with $C_j = \cos((j-1)\delta\theta)\cos(j\,\delta\theta)$ and $S_j = \sin((j-1)\delta\theta)\sin(j\,\delta\theta)$.

Assuming $x \to 0$ and $x\delta t \ll 1$ (but finite δt) we can write, up to a global phase,

$$V_j = \begin{pmatrix} C_j + S_j & iC_j x\delta t - \frac{S_j x}{2}(1 - e^{-2i\delta t}) \\ iC_j x\delta t - \frac{S_j x}{2}(1 - e^{-2i\delta t}) & C_j + S_j e^{-2i\delta t} \end{pmatrix}. \tag{8}$$

Further we consider $\delta\theta \ll 1$. There are special values of δt corresponding to $\exp(-2i\delta t) = 1$

$$\delta t = \pi k, \quad k = 1, 2, 3, \ldots, \tag{9}$$

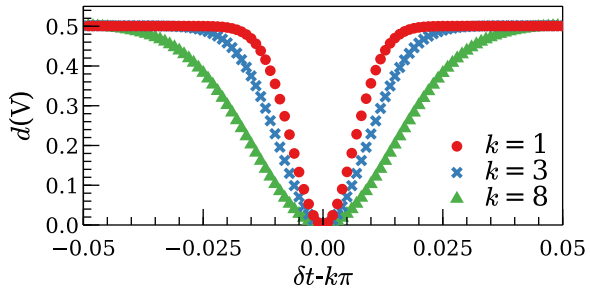

FIG. 5. Distance from unitarity for a complete process as a function of δt.

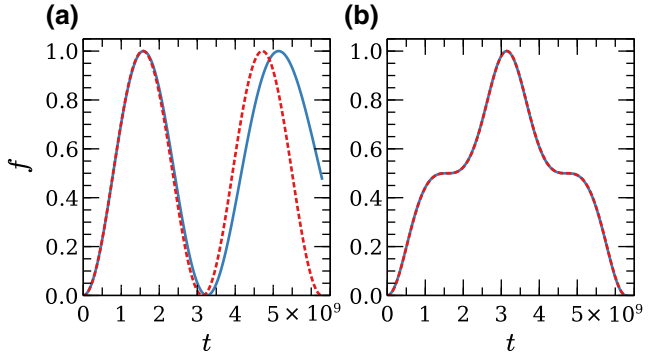

FIG. 6. Fidelity of matching target state versus the time with $N = 10^{18}$, $\delta t = 10^6\pi$, and $\delta\theta/\delta t = 0.1x$ for the solid line in (a) and $\delta\theta/\delta t = x$ for the solid line in (b). Dashed line in (a) corresponds to continuous Grover dynamics, Eq. (2). The dashed line in (b) is calculated using the approximation, Eq. (13), which shows perfect agreement with the direct simulation.

when each term V_j can be approximated by a rescaled unitary, hence the same will hold for the whole process $V(n)$.

As a measure of (non)unitarity we use the distance

$$d(V) = 1 - \frac{1}{2}\mathrm{Tr}(V^\dagger V) \tag{10}$$

employing the Frobenius norm. We can use this measure to track the tradeoff between the unitarity (i.e., quantum computation) and nonunitarity (i.e., classical computation) of the process.

To illustrate the analytical result, Eq. (9), we plot in Fig. 5 the dependence of $d(V)$ of the resulting transformation $V(n_G)$ (with $n_G = \lfloor \pi\sqrt{N}/(2\delta t)\rfloor$) for various values of δt with $N = 10^{10}$ and $\delta\theta/\delta t = 3\times 10^{-6}$. The minima can be determined from Eq. (9), which involves neither the parameter $\delta\theta$, nor the index j.

For further analysis let us define a non-Hermitian effective Hamiltonian $H_{\mathrm{eff}}(t)$ by taking the formula

$$V_j = e^{-iH_{\mathrm{eff}}(j\,\delta t)\delta t} \tag{11}$$

for each j, and extending $H_{\mathrm{eff}}(t)$ as piecewise constant on the intervals $((j-1)\delta t, j\,\delta t]$. The resulting time-dependent (non-Hermitian) Hamiltonian provides an equivalent description of the search algorithm.

Introducing the parameter τ, which describes the level of nonunitarity as $\delta t = \pi k + \tau$, for some integer k, and assuming $|\tau| \ll 1$ we can approximate the piecewise constant non-Hermitian Hamiltonian by the continuous expression

$$\begin{aligned} H_{\mathrm{eff}}(t) \approx & -x\cos^2(\alpha x t)\left(|w\rangle\langle r| + |r\rangle\langle w|\right) \\ & + 2\frac{\tau}{\delta t}\sin^2(\alpha x t)\,|r\rangle\langle r| - 2i\sin^2(\alpha x t)\frac{\tau^2}{\delta t}\,|r\rangle\langle r|, \end{aligned} \tag{12}$$

where $\alpha x = \delta\theta/\delta t$. We note that when $\tau = 0$ the right-hand side becomes Hermitian, thus the formal expression $V(n) \approx \mathcal{T}\exp(-i\int_0^{n\delta t} H_{\mathrm{eff}}(t')dt')$ permits an approximation by purely unitary dynamics,

$$\begin{aligned} V(n) &\approx \mathbb{I}\cos(A(n)) + i\left(|w\rangle\langle r| + |r\rangle\langle w|\right)\sin(A(n)), \\ A(n) &= \frac{x\delta t}{2}\left(n + \frac{\sin(2n\delta\theta)}{2\delta\theta}\right). \end{aligned} \tag{13}$$

Note, that in the limit $\delta\theta \to 0$ we have $A(n) = xn\delta t$, yielding the standard continuous Grover algorithm with $f(n) = \sin^2(xn\delta t)$. The first maximum occurs at time $T_0 = n_G\delta t = \pi\sqrt{N}/2$, while for $\delta\theta/\delta t = x$ the first maximum is reached at time $\pi\sqrt{N}$. In Fig. 6 we plot some numerical examples.

At nonzero values of τ we expect the non-Hermitian component to drive the system to a steady state. Of particular interest is the emergence of an asymptotic dynamics consisting of the target state $|w\rangle$ alone, manifesting in the saturation of the target fidelity at the value of 1. A heuristic analysis of the Hamiltonian (12) shows that in order to achieve saturation dynamics of the fidelity, the relation $\sqrt{x\delta t} \ll \tau \ll 1$ must hold between control parameters (see Appendix for details).

It is worth pointing out that in our algorithm, when we choose $\theta_0 = \pi/4$ and $\delta t = \pi/2 + \pi k$, $k = 0, 1, 2, \ldots$, the first iteration of our algorithm may be approximately described via $V_1 \approx |w\rangle\langle w|$ (up to corrections of order $x\delta t \ll 1$). In this situation we would have a *classical search regime*, i.e., we can organize *projection onto the unknown state* $|w\rangle$, and the probability of a successful outcome of the ancilla measurement for initial state $|s\rangle$ is $\langle s|V_1^\dagger V_1|s\rangle \approx 1/N$, which corresponds to the efficiency of the classical search $O(N)$. This example demonstrates the possibility of a classical computation regime, which is the opposite of the quantum limit discussed after Eq. (13).

Thus we show that the proposed algorithm contains quantum, classical, and intermediate regimes depending on the parameters chosen.

IV. SCALING PROPERTIES

To study the scaling properties of our nonunitary dynamics we investigate the following transformation of Hamiltonian (12): $xt = t'$, $H'(t') = H(t)/x$ while keeping $x\delta t$ and τ constant, and assuming $x\delta t \ll 1$. The last condition here can be approximately satisfied by properly choosing both $N \gg 1$ and an integer k. If we have $V(n)$ for some $N = N_1$ and $\delta t_1 = k_1\pi + \tau$, then we can find $N_2 > N_1$ and $\delta t_2 = k_2\pi + \tau$, which corresponds to approximately the same operator $V(n)$ when k_2 is an integer such that

$$k_2 \approx \frac{1}{\pi}\sqrt{\frac{N_2}{N_1}}(k_1\pi + \tau) - \frac{\tau}{\pi}. \tag{14}$$

This means that we have almost the same number of steps of the protocol for different N, and the duration δt of each step is proportional to $\sqrt{N}$. As can be seen, the needed relative accuracy of timing $\tau/\delta t \propto 1/\sqrt{N}$ grows with N.

The recurrence relation, Eq. (14), can be used to characterize the scaling properties of the algorithm. Assume that we have a certain process with fidelity $f_1(t)$, survival probability $P_1(t)$, and this process is characterized by N_1, δt_1, and $\delta\theta_1$. We argue that for any requested database size $N_r \gg N_1$ we can find database size $N_2 \geq N_r$ with corresponding parameters δt_2, $\delta\theta_2$ to have another process with $f_2(t)$ and $P_2(t)$, which is an approximately time-scaled copy of the first process with $\delta t_2 \approx \delta t_1\sqrt{N_2/N_1}$:

$$f_2(t) \approx f_1(t\sqrt{N_2/N_1}), \tag{15}$$

$$P_2(t) \approx P_1(t\sqrt{N_2/N_1}), \tag{16}$$

$$N_2 = \left\lceil N_1 \left(\frac{\pi\left\lceil \frac{1}{\pi}\sqrt{\frac{N_r}{N_1}}(k_1\pi + \tau) - \frac{\tau}{\pi}\right\rceil + \tau}{\pi k_1 + \tau}\right)^2 \right\rceil, \tag{17}$$

and as can be seen $N_2/N_r \to 1$ with $N_r/N_1 \to \infty$.

For a numerical example we choose $N = 10^6$ and $\alpha = 0.3$, $\tau = 0.2$, $k = 1$, $\delta t = k\pi + \tau$ as a reference process, which gives desired $V(n)$. Using Eq. (17) we find larger database size ($N_r = 10^{18}$), and corresponding integer value of the parameter k, which gives the same $V(n_G)$ as our reference process ($n_G = \lfloor \pi\sqrt{N}/(2\delta t)\rfloor$ is the number of steps corresponding to T_0). The resulting processes are depicted in Fig. 7. Note, the expression (14) is not satisfied exactly for the process (b) in Fig. 7. For requested $N_r = 10^{18}$ we have $N_2 = 1.000\,000\,162\,505\,052\,417 \times 10^{18}$, and from Eq. (14) we have $k_2 = 1\,063\,662.000\,000\,000\,2$, however we can see that $k_2 - \lfloor k_2\rfloor \ll 1$, and for our particular choice we have $k_2 - \lfloor k_2\rfloor \ll \tau$. Processes depicted in Fig. 7 have almost the same survival probability $P(n_G) \approx 0.27$ and $f(n_G) \approx 0.98$. At last, the chosen numerical parameters satisfy the condition for saturation dynamics, which is discussed in the previous section: $\sqrt{x\delta t} \ll \tau \ll 1$ (as well as $0.06 \ll 0.2 \ll 1$), and we can see from Fig. 7 that our nonunitary process shows saturation and has an attractor $|w\rangle$.

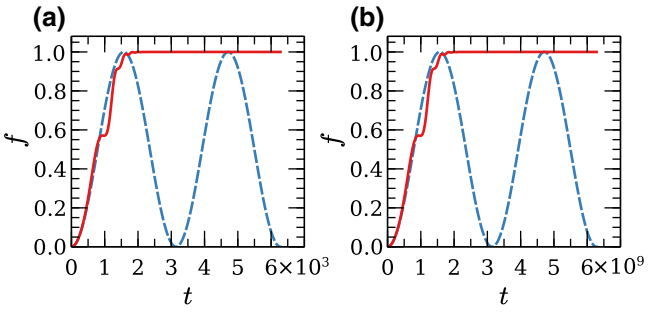

FIG. 7. Illustration of the scalability of the proposed algorithm. We show the fidelity of matching target state versus the time for common Grover algorithm (dotted line) and nonunitary search (solid lines) with $\alpha = 0.3$ and $\tau = 0.2$. (a) $N = 10^6$, $k = 1$ (b) $N = 1.000\,000\,162\,505\,052\,417 \times 10^{18}$, $k = 1.063\,662 \times 10^6$.

To provide some insight into the the features observed in Fig. 7, we plot the success probabilities p_n for each step n in Fig. 8. We emphasize that at the beginning of the evolution, the success probabilities are relatively far below unity, which indicates that this process cannot be categorized as a standard QZE. However, in the saturation regime, we obtain $p_n \to 1$, hence the process becomes more Zeno-like.

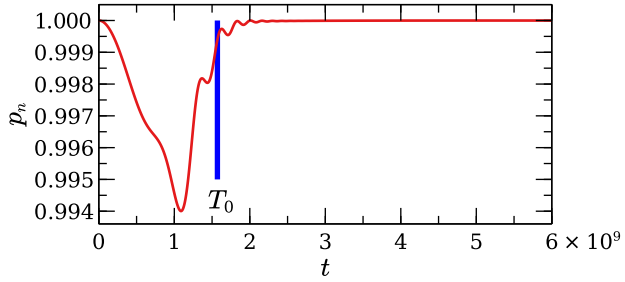

FIG. 8. Success probability of a single step of the computation process as a function of time, with parameters corresponding to Fig. 7(b). In saturation regime we have $p_n \to 1$. $T_0 \approx 1.57 \times 10^9$.

V. ROBUSTNESS AGAINST ORACLE DETUNING ERROR

The continuous-time-search algorithm requires a high level of accuracy. For instance, if we have a detuned oracle [40] described by

$$H_o^{(\varepsilon)} = (1+\varepsilon)H_o, \tag{18}$$

then the fidelity of the output state $f\,(t) = |\,\langle w|U(t)|s\rangle\,|^2$ can be low even for $|\varepsilon| \ll 1$ (see, e.g., Refs. [26,40]).

This section is dedicated to the study of the performance of the nonunitary algorithm under the effect of two kinds of detuning errors. In both scenarios, we consider the procedure of stopping the evolution (calculation) at time T_0 or step n_G, for the Hamiltonian and the nonunitary algorithms, respectively, which would yield optimal search performances if the systems were free of errors.

Our first study concerns the static detuning of the oracle Hamiltonian, i.e., when ε has some fixed unknown value. It has been shown that stopping the evolution after the Grover time T_0 completely fails if the error parameter satisfies a "resonance condition" $\varepsilon = \pm 2x\sqrt{4m^2-1}$, for integer m [26], and behaves unfavorably in the neighborhoods of these points. We carried out numerical simulations of both the original and the nonunitary search algorithm with parameters corresponding to (b) in Fig. 7 and using two different values of ε satisfying the "resonance condition:" $\varepsilon = 2x\sqrt{3}$ and $\varepsilon = 2x\sqrt{15}$. For comparison, in Fig. 9 we plot the fidelity given by the original search Hamiltonian (f_G), the target fidelity of our nonunitary algorithm (f), as well as the target fidelity f_{eff} given by the approximate effective non-Hermitian Hamiltonian description. The latter case corresponds to extending the Hamiltonian in Eq. (12) by an additional term corresponding to the oracle error: $H_{\text{eff}}(t) \to H_{\text{eff}}(t) - \varepsilon\,|w\rangle\,\langle w|$. The thick vertical line in Fig. 9 indicates the readout step n_G chosen obliviously to the error parameter ε. We have $P(n_G) \approx 0.08, f\,(n_G) \approx 0.88$ for $m = 1$, and $P(n_G) \approx 0.018$, $f\,(n_G) \approx 0.63$ for $m = 2$.

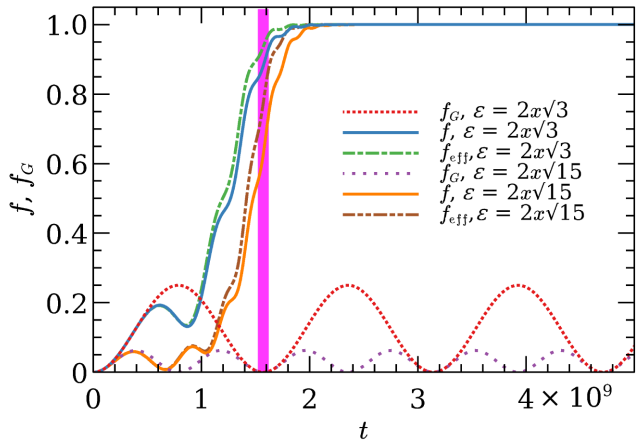

FIG. 9. Exact fidelity f and approximate fidelity f_{eff} calculated using non-Hermitian Hamiltonian (12) for nonunitary process, and fidelity f_G for unitary Grover search as functions of time for two different values of detuning ε. The vertical solid line corresponds to the time moment when the final measurement is performed.

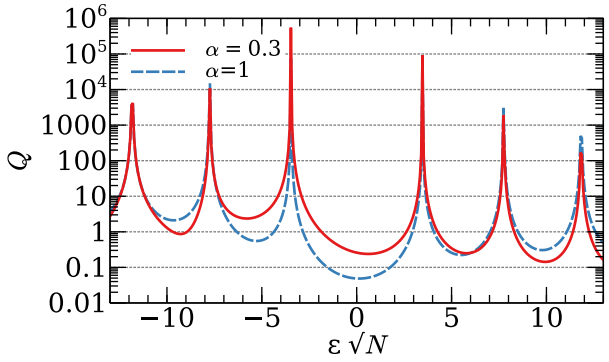

FIG. 10. The Q factor versus oracle detuning ε for $N = 10^{18}$, $\delta t = 10^6\pi + \tau$, $\tau = 0.2$. Peaks correspond to the "resonance condition."

In order to compare the performance of our nonunitary protocol with continuous Grover search, let us introduce the "quality factor" $Q = f\,(n_G)P(n_G)/f_G(\pi/2x)$. As can be seen, $Q > 1$ ($Q < 1$) corresponds to the case when our proposed nonunitary algorithm is better (worse) than the standard Grover algorithm (we assume that measurements are instantaneous). In Fig. 10 we show the dependence of Q as a function of the systematic oracle error ε. As can

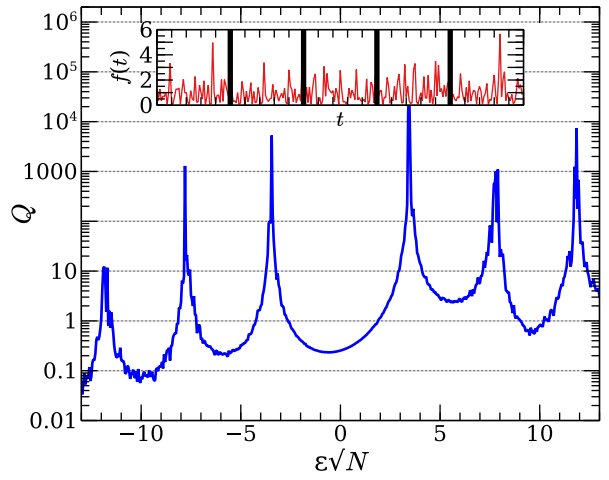

FIG. 11. The Q factor versus strength of the noise ε in control for $N = 10^{18}$, $\delta t = 10^6\pi + \tau$, $\tau = 0.2$, $\alpha = 0.3$. In the inset the biased white-noise example is shown. Vertical solid lines correspond to the ancilla measurements, and a single realization of the noisy process is made for each value of ε. Noise function $f\,(t)$ is modeled by rectangle pulses with duration $\delta t/50$ and amplitude $-\log(R)$, where R is a uniform random number from interval $(0, 1)$.

be seen, there is a set of intervals of ε values where our nonunitary algorithm fares clearly better than the standard continuous-search algorithm.

Now we turn to the analysis of the time-dependent detuning of the oracle, or a noisy driving of the Hamiltonian. In particular, instead of Eq. (3) we consider the following Hamiltonian:

$$H^{(\mathrm{noisy})}(t) = -\mathcal{I} \otimes |w\rangle \langle w| - (1 + \varepsilon f(t))\sigma_z \otimes |s\rangle \langle s|, \tag{19}$$

where the noise function $f(t)$ has a mean value of $\overline{f(t)} = 1$. Our numerical results for the Q value are displayed in Fig. 11 we plot the Q value for the case of noisy control with $f(t)$ modeled as a biased white noise (see inset of Fig. 11). As can be seen, the improvement in robustness is similar to that of constant detuning, shown in Fig. 10.

VI. RELATIONS TO OTHER ALGORITHMS USING MEASUREMENT

While our algorithm resembles the standard quantum Zeno effect in that frequent measurements are carried out on the dynamical system and the continuation of the evolution is conditioned upon a correct measurement outcome [41], there are significant differences. The quantum Zeno effect can be observed when the survival probability at each measurement can be engineered to be arbitrarily close to unity, yielding a process that shares many features with adiabatic processes [42]. As a consequence, given a unitary evolution and projective measurements, the resulting Zeno dynamics in a restricted subspace becomes unitary as well. The quantum Zeno effect in quantum computing has found applications such as error correction [43] and algorithm design [2,4,5]. Common to these algorithmic applications is that the database registers are measured to induce the Zeno dynamics, while our algorithm uses measurements of the ancilla only. The quantum circuits studied in Refs. [2,5] operate in the regime where the survival probability at each iteration is kept arbitrarily close to unity, thereby operating in the standard quantum Zeno regime.

The notion of bomb query complexity introduced by Lin *et al.* [5] showed a remarkable relation between Zeno dynamics and quantum query complexity, namely that the former is quadratically worse than the latter. However, since observation can lead to more complex dynamics [44], this result appears to be specific to the simple measurement scheme and coupling between the ancilla and the oracle operation. As an example, we show here that our algorithm can retain the scaling of the quantum search algorithm.

Closest in spirit to our algorithm is the reported quantum search algorithm based on counterfactual quantum computing [4]. Both approaches start with less than 1 survival probabilities in the initial iterations and quickly converge to a regime where the required measurement outcome is obtained with almost certainty, while exhibiting robustness against certain errors. The counterfactual search, however, suffers from a conceptual [45] and several technical drawbacks that our approach avoids. Namely, it requires the implementation of both the oracle and its adjoint, and it might be strongly affected by systematic errors in the oracle. In addition, no scalable analysis is presented in the paper, therefore it is not clear how the nonunit survival probability scales with the database size.

Finally, while the algorithm combining adiabatic quantum search by measurement employs a rather similar idea of coupling to an ancilla [3], it uses a term $H_o \otimes p$, which is physically very nontrivial. In contrast, our coupling term is completely oblivious to the marked node.

VII. DISCUSSION AND CONCLUSION

In the case without detuning of the oracle, both the success probability of each step and the target fidelity are approaching 1 (see solid lines in Figs. 7 and 8). The saturation of the success probability makes the algorithm ideal for applications where verification queries to the classical database are impossible or come at a high cost. While the algorithm carries strong similarities with the quantum Zeno effect [46,47], and is based on the approach and techniques of Zeno-like dynamics in specific physical systems [12,14,16] it employs a time-dependent sequence of projections (via parameter θ_n). The protocol therefore shows similarities also with the proposal of von Neumann to transform quantum states by measurement [48], but in our protocol the final state is selected by the oracle Hamiltonian.

The synergy of quantum and classical computation in our algorithm is the result of selective measurements of the ancilla. The classical contribution in the efficiency Q defined above is determined by the probability $P \leq 1$ (in pure quantum case $P = 1$). The quantum:classical ratio of the algorithm can be tuned by properly choosing time intervals δt between subsequent measurements. We note that our algorithm involves only a single quantum process, differing from studies considering the combined application of quantum and classical computers [49].

In summary, we present a resource-efficient and robust nonunitary modification of the continuous version of Grover's search based on measurements and conditional evolution. We show that this dynamics can be accurately described by a non-Hermitian effective Hamiltonian in the Hilbert space $\mathcal{H}_N$, and determined its scaling properties under ideal conditions.

There are many possible directions for further development of similar protocols. For instance, the driven part of the Hamiltonian, the parameters δt and $\delta\theta$ can be made time dependent (see, e.g., Ref. [50]). We believe that the presented protocol will serve for a better

understanding of controllable nonunitary processes and their scaling properties.

ACKNOWLEDGMENTS

P.V.P. and A.G. are supported by the National Research, Development and Innovation Office of Hungary (NKFIH) Project No. K124351; P.V.P. by NKFIH through the Projects No. K115624, No. PD120975, No. 2017-1.2.1-NKP-2017-00001; and A.G. by MŠMT RVO 14000. P.V.P. and L.A.W. are supported by Grant No. PGC2018-101355-B-I00 funded by MCIN/AEI/10.13039/501100011033 and by "ERDF A way of making Europe". L.A.W. is supported by the Grant No. PID2021-126273NB-I00 funded by MCIN/AEI/10.13039/501100011033, and the Basque Government through Grant No. IT1470-22. J.Q.Y. is supported by the National Natural Science Foundation of China (Grant No. 11934010).

APPENDIX: CONDITION FOR SATURATION BEHAVIOR OF THE TARGET FIDELITY

We employ the following heuristic analysis to estimate the ranges of parameters as well as the convergence time. Instead of Eq. (12) we consider the following non-Hermitian time-independent Hamiltonian:

$$h = h_0 - i\gamma \, |r\rangle \, \langle r| \, , \tag{A1}$$

where $h_0 = -x(|w\rangle \, \langle r| + |r\rangle \, \langle w|)$ and $x > 0$, $\gamma > 0$. We can write the non-normalized general solution of Schrödinger equation as

$$|\psi(t)\rangle = \sum_n e^{-i\epsilon_n t} \, \langle \chi_n | \psi(0)\rangle \, |\varphi_n\rangle \, , \tag{A2}$$

where $h \, |\varphi_n\rangle = \epsilon_n \, |\varphi_n\rangle$, $h^\dagger \, |\chi_n\rangle = \lambda_n \, |\chi_n\rangle$, $\langle \chi_n | \varphi_m \rangle = \delta_{nm}$, $\epsilon_n = \lambda_n^*$, and $|\psi(0)\rangle = |s\rangle$ is the initial state. One can see that in the limit $\gamma \gg x$ we have $\epsilon_1 \approx -ix^2/\gamma \to 0$, $\epsilon_2 \approx -i\gamma$, and thus for $t \gg \gamma^{-1}$ we have $|\psi(t)\rangle \approx e^{-x^2 t/\gamma} \, \langle \chi_1 | \psi(0)\rangle \, |\varphi_1\rangle$ with $\langle \chi_1 | \psi(0)\rangle \approx -x/\gamma$ and $|\varphi_1\rangle \approx (1; \, -ix/\gamma)^T (1 + (x/\gamma)^2)^{-1/2}$.

In other words, we have a saturation where the state approximates approaches $|w\rangle$ state when $x \ll \gamma$ and $t > x^{-1}$ with target fidelity $|\langle w|\psi(t)\rangle|^2 \propto x^2 = 1/N$, which corresponds to the classical search efficiency. By turning off damping $\gamma \to 0$ we can achieve a unitary process with quantum efficiency. The Hamiltonian in Eq. (12) is non-Hermitian and time dependent and its complete analysis is complicated (see, e.g., Refs. [51,52]). In order to have a general picture of the role of control parameters we collate our simple example with Eq. (12) and approximately set $\gamma \approx \tau^2/\delta t$. Thus we can expect saturation regime in the case $\tau \gg \sqrt{x\delta t}$. By definition τ has a finite value, and moreover, we assume $\tau \ll 1$ while we derive Eq. (12), thus we have to choose

$$\sqrt{x\delta t} \ll \tau \ll 1 \tag{A3}$$

in order to have saturation property of the computation process.

This requirement also does not contradict our assumption $x\delta t \ll 1$, which is made in the main text. Actually, this assumption has a clear physical meaning: we have to make many measurement cycles during the common Grover time T_0 defined earlier. Finally, if $\sqrt{x\delta t} \gg \tau \to 0$ we do not have a saturation because the process becomes close to unitary.

[1] P. Facchi and S. Pascazio, Quantum zeno dynamics: Mathematical and physical aspects, J. Phys. A: Math. Theor. **41**, 493001 (2008).
[2] T. Rudolph and L. Grover, Quantum searching a classical database (or how we learned to stop worrying and love the bomb), ArXiv:quant-ph/0206066v (2002).
[3] A. M. Childs, E. Deotto, E. Farhi, J. Goldstone, S. Gutmann, and A. J. Landahl, Quantum search by measurement, Phys. Rev. A **66**, 032314 (2002).
[4] O. Hosten, M. T. Rakher, J. T. Barreiro, N. A. Peters, and P. G. Kwiat, Counterfactual quantum computation through quantum interrogation, Nature **439**, 949 (2006).
[5] C. Y.-Y. Lin and H.-H. Lin, in *30th Conference on Computational Complexity (CCC 2015)*, Leibniz International Proceedings in Informatics (LIPIcs), Vol. 33, edited by D. Zuckerman (Schloss Dagstuhl–Leibniz-Zentrum fuer Informatik, Dagstuhl, Germany, 2015), p. 537.
[6] A. Gilyén, Y. Su, G. H. Low, and N. Wiebe, in *Proceedings of the 51st Annual ACM SIGACT Symposium on Theory of Computing*, STOC 2019 (Association for Computing Machinery, Phoenix, AZ, USA, 2019), p. 193.
[7] E. Knill, R. Laflamme, and G. J. Milburn, A scheme for efficient quantum computation with linear optics, Nature **409**, 46 (2001).
[8] H. Terashima and M. Ueda, Nonunitary quantum circuit, Int. J. Quantum Inf. **03**, 633 (2005).
[9] V. Kendon and B. C. Sanders, Complementarity and quantum walks, Phys. Rev. A **71**, 022307 (2005).
[10] V. Kendon and O. Maloyer, Optimal computation with non-unitary quantum walks, Theor. Comput. Sci. **394**, 187 (2008), from Gödel to Einstein: Computability between Logic and Physics.
[11] N. Usher, M. J. Hoban, and D. E. Browne, Nonunitary quantum computation in the ground space of local hamiltonians, Phys. Rev. A **96**, 032321 (2017).
[12] H. Nakazato, T. Takazawa, and K. Yuasa, Purification Through Zeno-Like Measurements, Phys. Rev. Lett. **90**, 060401 (2003).
[13] L.-A. Wu, D. A. Lidar, and S. Schneider, Long-range entanglement generation via frequent measurements, Phys. Rev. A **70**, 032322 (2004).
[14] Y. Li, L.-A. Wu, Y.-D. Wang, and L.-P. Yang, Nondeterministic ultrafast ground-state cooling of a mechanical resonator, Phys. Rev. B **84**, 094502 (2011).

[15] P. V. Pyshkin, D.-W. Luo, J. Q. You, and L.-A. Wu, Ground-state cooling of quantum systems via a one-shot measurement, Phys. Rev. A **93**, 032120 (2016).

[16] P. V. Pyshkin, E. Y. Sherman, and L.-A. Wu, Polaron formation in a spin chain by measurement-induced imaginary zeeman field, Phys. Rev. B **104**, 075136 (2021).

[17] I. A. Luchnikov and S. N. Filippov, Quantum evolution in the stroboscopic limit of repeated measurements, Phys. Rev. A **95**, 022113 (2017).

[18] A. Streltsov, H. Kampermann, and D. Bruß, Linking Quantum Discord to Entanglement in a Measurement, Phys. Rev. Lett. **106**, 160401 (2011).

[19] A. Gilyén, T. Kiss, and I. Jex, Exponential sensitivity and its cost in quantum physics, Sci. Rep. **6**, 20076 (2015).

[20] P. J. Coles and M. Piani, Complementary sequential measurements generate entanglement, Phys. Rev. A **89**, 010302(R) (2014).

[21] J. M. Torres, J. Z. Bernád, G. Alber, O. Kálmán, and T. Kiss, Measurement-induced chaos and quantum state discrimination in an iterated Tavis-Cummings scheme, Phys. Rev. A **95**, 023828 (2017).

[22] P. V. Pyshkin, D.-W. Luo, J. Q. You, and L.-A. Wu, Nondeterministic quantum computation via ground state cooling and ultrafast Grover algorithm, ArXiv arXiv:1704.01467 (2017).

[23] R. Grimaudo, A. Messina, A. Sergi, N. V. Vitanov, and S. N. Filippov, Two-qubit entanglement generation through non-Hermitian Hamiltonians induced by repeated measurements on an ancilla, Entropy **22**, 1184 (2020).

[24] M. H. S. Amin, P. J. Love, and C. J. S. Truncik, Thermally Assisted Adiabatic Quantum Computation, Phys. Rev. Lett. **100**, 060503 (2008).

[25] D.-W. Luo, P. V. Pyshkin, C.-H. Lam, T. Yu, H.-Q. Lin, J. Q. You, and L.-A. Wu, Dynamical invariants in a non-Markovian quantum-state-diffusion equation, Phys. Rev. A **92**, 062127 (2015).

[26] L. Novo, S. Chakraborty, M. Mohseni, and Y. Omar, Environment-assisted analog quantum search, Phys. Rev. A **98**, 022316 (2018).

[27] E. Farhi and S. Gutmann, Analog analogue of a digital quantum computation, Phys. Rev. A **57**, 2403 (1998).

[28] L.-A. Wu and M. S. Byrd, Self-protected quantum algorithms based on quantum state tomography, Quantum Inf. Process. **8**, 1 (2008).

[29] D. A. Lidar and L.-A. Wu, Encoded recoupling and decoupling: An alternative to quantum error-correcting codes applied to trapped-ion quantum computation, Phys. Rev. A **67**, 032313 (2003).

[30] E. Farhi, J. Goldstone, S. Gutmann, and M. Sipser, Quantum computation by adiabatic evolution, eprint arXiv:quant-ph/0001106 (2000).

[31] J. Roland and N. J. Cerf, Quantum search by local adiabatic evolution, Phys. Rev. A **65**, 042308 (2002).

[32] A. Pérez and A. Romanelli, Nonadiabatic quantum search algorithms, Phys. Rev. A **76**, 052318 (2007).

[33] F.-G. Li, W.-S. Bao, T. Li, H. liang Huang, S. Zhang, and X.-Q. Fu, Nonadiabatic quantum search algorithm with analytical success rate, Int. J. Theor. Phys. **58**, 939 (2018).

[34] M. Salerno, The Hubbard model on a complete graph: Exact analytical results, Z. Phys. B Condens. Matter **99**, 469 (1995).

[35] A. C. Jacko, A. L. Khosla, J. Merino, and B. J. Powell, Spin-orbit coupling in $Mo_3S_7(dmit)_3$, Phys. Rev. B **95**, 155120 (2017).

[36] S. Lloyd, Universal quantum simulators, Science **273**, 1073 (1996).

[37] L.-A. Wu, M. S. Byrd, and D. A. Lidar, Polynomial-Time Simulation of Pairing Models on a Quantum Computer, Phys. Rev. Lett. **89**, 057904 (2002).

[38] A. Smith, M. S. Kim, F. Pollmann, and J. Knolle, Simulating quantum many-body dynamics on a current digital quantum computer, Npj Quantum Inf. **5**, 106 (2019).

[39] F. Tacchino, A. Chiesa, S. Carretta, and D. Gerace, Quantum computers as universal quantum simulators: State-of-the-art and perspectives, Adv. Quantum Technol. **3**, 1900052 (2020).

[40] N. Shenvi, K. R. Brown, and K. B. Whaley, Effects of a random noisy oracle on search algorithm complexity, Phys. Rev. A **68**, 052313 (2003).

[41] P. Facchi and S. Pascazio, Quantum Zeno dynamics: Mathematical and physical aspects, J. Phys. A: Math. Theor. **41**, 493001 (2008).

[42] D. Burgarth, P. Facchi, H. Nakazato, S. Pascazio, and K. Yuasa, Generalized adiabatic theorem and strong-coupling limits, Quantum **3**, 152 (2019).

[43] G. A. Paz-Silva, A. T. Rezakhani, J. M. Dominy, and D. A. Lidar, Zeno Effect for Quantum Computation and Control, Phys. Rev. Lett. **108**, 080501 (2012).

[44] D. K. Burgarth, P. Facchi, V. Giovannetti, H. Nakazato, S. Pascazio, and K. Yuasa, Exponential rise of dynamical complexity in quantum computing through projections, Nat. Commun. **5**, 5173 (2014).

[45] G. Mitchison and R. Jozsa, The limits of counterfactual computation, ArXiv:quant-ph/0606092v3 (2006).

[46] B. Misra and E. C. G. Sudarshan, The Zeno's paradox in quantum theory, J. Math. Phys. **18**, 756 (1977).

[47] P. Exner, *Open Quantum Systems and Feynman Integrals*, Fundamental Theories of Physics (Springer Netherlands, 1985).

[48] J. von Neumann, *Mathematical Foundations of Quantum Mechanics* (Princeton Univ Press, Princeton, 1955), p. 365.

[49] S. Bravyi, G. Smith, and J. A. Smolin, Trading Classical and Quantum Computational Resources, Phys. Rev. X **6**, 021043 (2016).

[50] F. Wilczek, H.-Y. Hu, and B. Wu, Resonant quantum search with monitor qubits, Chin. Phys. Lett. **37**, 050304 (2020).

[51] G. Dattoli, A. Torre, and R. Mignani, Non-Hermitian evolution of two-level quantum systems, Phys. Rev. A **42**, 1467 (1990).

[52] B. Bagchi, Evolution operator for time-dependent non-Hermitian Hamiltonians, Lett. High Energy Phys. **1**, 4 (2018).